South-Western Institute for Astronomy Research
Yunnan University

Weak lensing cosmology beyond two-point shear correlations

Zuhui Fan
(SWIFAR, Yunnan University)

Dec. 15, 2023 @ 32nd Texas Symposium

Outline

- Introduction
- Weak lensing peak statistics – from modeling to application
  - Peak height
  - IA impact
  - Peak steepness
- Shear-magnification (galaxy number density) cross correlations
- Summary

- **Introduction**

Weak lensing effects

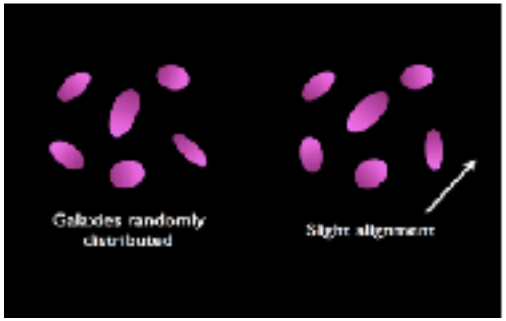

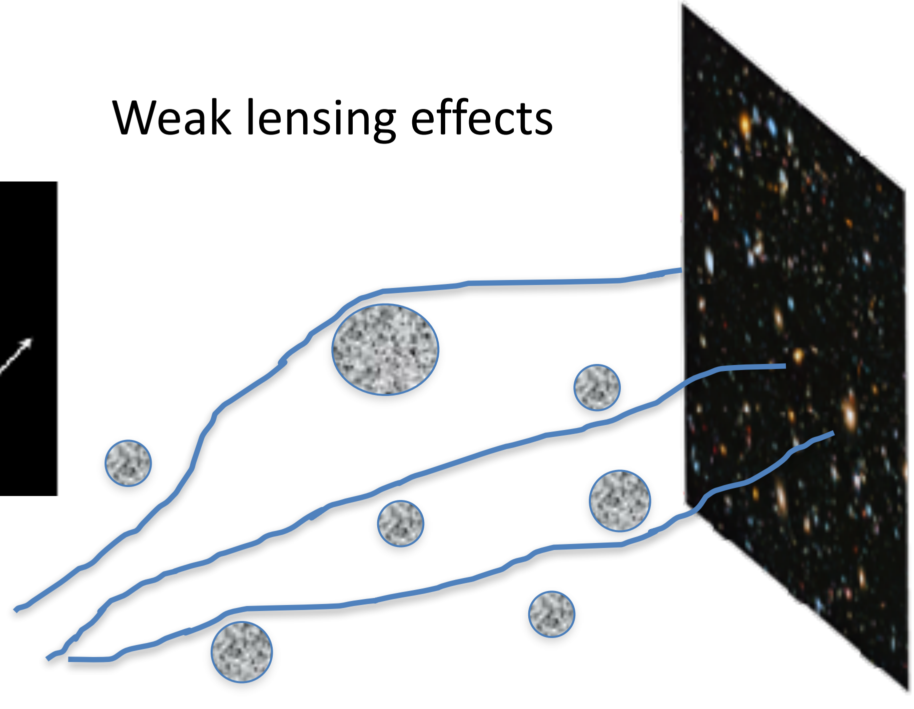

Arising from gravitational light deflections by large-scale structures, weak lensing effects are uniquely important in probing the dark components of the universe that currently dominate the cosmic matter composition.

Cosmic shear signals are at the percent level
→accurate measurements of a large sample of distant galaxies
→Statistical in nature

The developments of observing facilities with large FoV and megapixel CCD detectors have revolutionized imaging surveys, allowing us to accurately measure the shapes of far-away galaxies

→ **Weak lensing cosmology**

First cosmic shear detections in ~2000

Stage II surveys CFHTLens

- ~150deg^2
- ~10^6 galaxies
- Feasibility

Stage III surveys, DES, KIDS, HSC

- ~ N*10^3 deg^2
- ~10$^{7-8}$ galaxies
- Deliver important cosmological constraints

Now

Stage IV surveys, Euclid, Roman, CSST LSST

- ~ N*10^4 deg^2
- ~10^9 galaxies
- High precision cosmology

Coming soon

Statistical analyses – cosmic shear 2pt is the primary statistics
(3×2pt: cosmic shear+ galaxy clustering +galaxy-galaxy lensing)
Extensive studies about different systematics

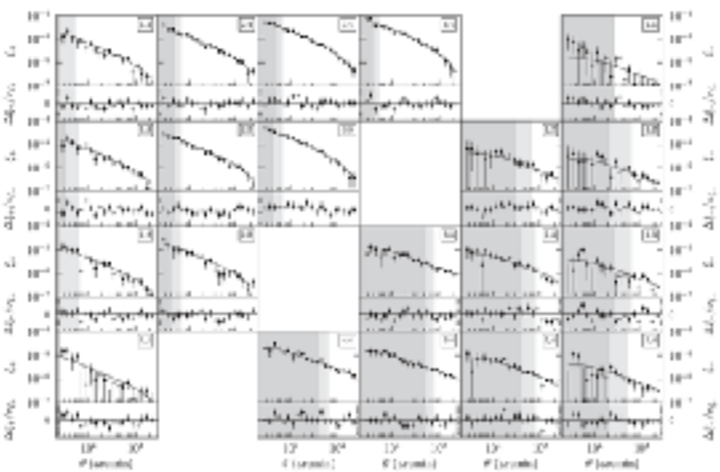

Abbott et al. 2022 (DES Y3)

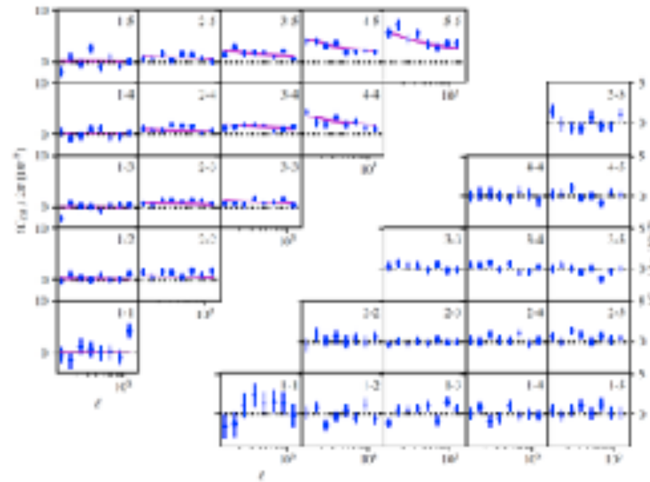

Heymans et al. 2021 (KiDS 1000)

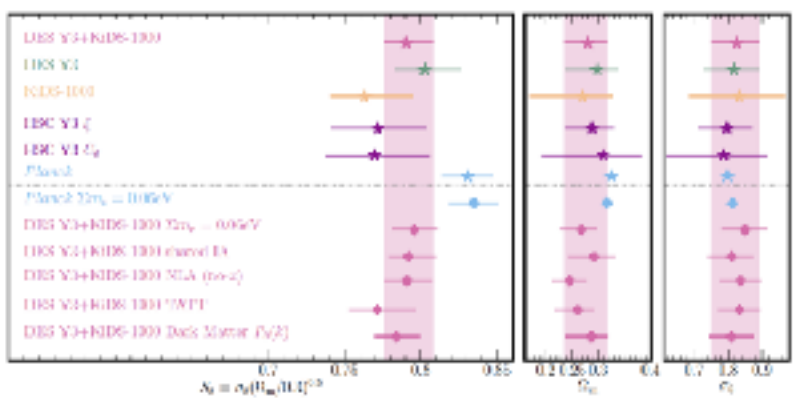

Abbott et al. 2023, DES Y3+KiDS-1000

Because of the non-Gaussian nature of the cosmic structures, statistics beyond the two-point analyses are needed to fully explore the cosmological Information embedded in the WL data

3pt correlation. (e.g., Fu et al. 2014, Burger et al. 2023)
Higher order CDF (e.g., Anbajagane et al. 2023)
Minkowski functionals (e.g., Grewal et al. 2022)
Machine learning (e.g., Ribli et al. 2019)
Scattering transformation (e.g., Cheng & Menard 2021)
......

Peak statistics (e.g., Liu,X. et al. 2015, Liu,J. et al. 2015, Liu, X. et al. 2016, Kacprzak et al. 2016, Martinet et al. 2018, Shan et al. 2018, Zurcher et al. 2022, Liu,X. et al. 2023)

- **Weak lensing peak statistics**

LOS matter concentrations (×lensing efficiency) → high WL signals → peaks in the WL mass maps → nonlinear and non-Gaussian features → cosmological inferences

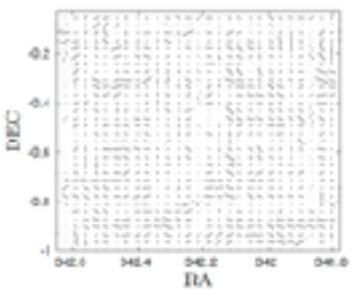

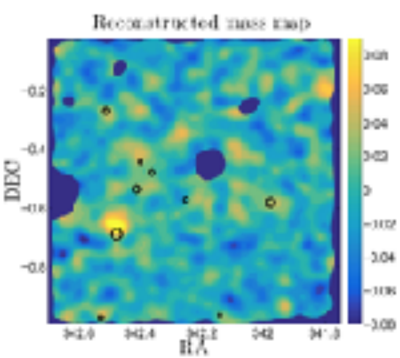

Liu,X. et al. 2015

To predict the cosmological dependences

Run large sets of simulations to build numerical templates

e.g., Zurcher et al. 2022, DES Y3

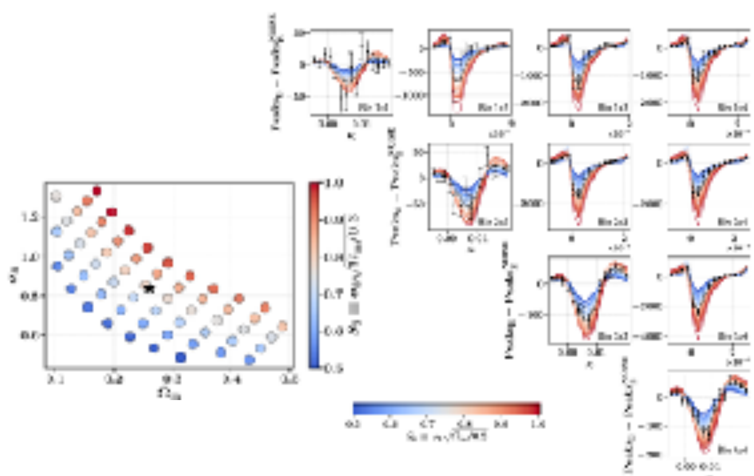

Incorporate theoretical modeling – our approach -- valid for high peaks

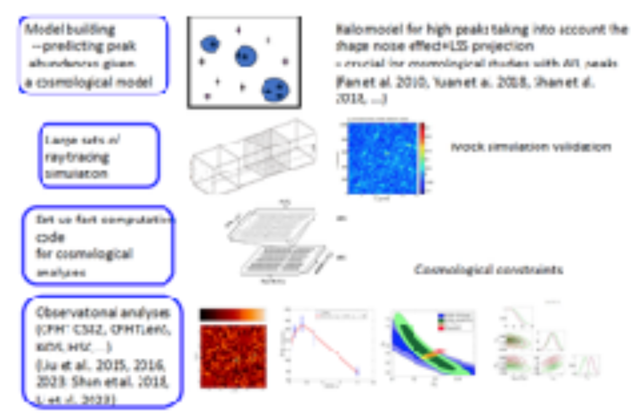

Theoretical model – Halo based (Fan et al. 2010, Yuan et al. 2018)

Assumption: Massive halos contribute dominantly to WL peaks ($M \geq M_* \sim 10^{14} h^{-1} M_{sun}$)

→ valid for high peaks

Including the shape noise and the LSS projection effects

→ adopt Gaussian approximatio

$$K = K_H + K_{LSS} + N \qquad n_{peak}(\nu)d\nu = n^c_{peak}(\nu)d\nu + n^n_{peak}(\nu)d\nu$$

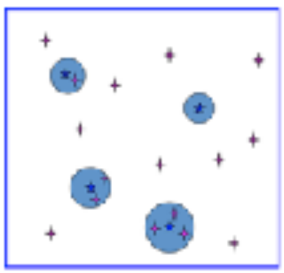

$$n^c_{peak}(\nu) = \int dz \frac{dV(z)}{dz d\Omega} \int_{M_*}^{\infty} dM\, n(M, z) \times \int_0^{\theta_{vir}} d\theta (2\pi\theta) \hat{n}^c_{peak}(\nu, M, z, \theta)$$

$$\hat{n}^c_{peak}(\nu, M, z, \theta) = \exp\left[-\frac{(K^1_H)^2 + (K^2_H)^2}{\sigma_1^2}\right] \times \left[\frac{1}{2\pi\theta_*^2} \frac{1}{(2\pi)^{1/2}}\right] \exp\left[-\frac{1}{2}\left(\nu - \frac{K_H}{\sigma_0}\right)^2\right] \times \int_0^{\infty} dx \left\{\frac{1}{[2\pi(1-\gamma^2)]^{1/2}} \times \exp\left[-\frac{[x + (K^{11}_H + K^{22}_H)/\sigma_2 - \gamma(\nu - K_H/\sigma_0)]^2}{2(1-\gamma^2)}\right] \times F(x)\right\}$$

$$n^n_{peak}(\nu) = \frac{1}{d\Omega} \times \left\{n_{ran}(\nu)\left[d\Omega - \int dz \frac{dV(z)}{dz} \int_{M_*}^{\infty} dM\, n(M, z)(\pi\theta^2_{vir})\right]\right\}$$

Cosmological information: halo profile and mass function, LSS, distance and volume

Extendable to include systematics into the model → photo-z errors, shear measurement errors, dilution effect, baryonic effects, IA effect, …

Applied to different surveys to derive cosmological constraints and test MG theories (Liu et al. 2015, 2016, 2023, Shan et al. 2018)

- **Cosmological constraints from HSC-SSP tomographic WL peak abundances**

First-year shear catalog (S16A) (Liu et al. 2023)

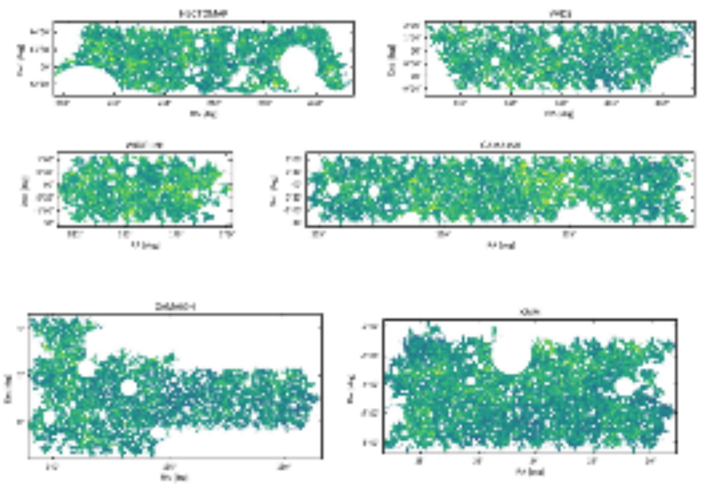

Mandelbaum et al. 2018

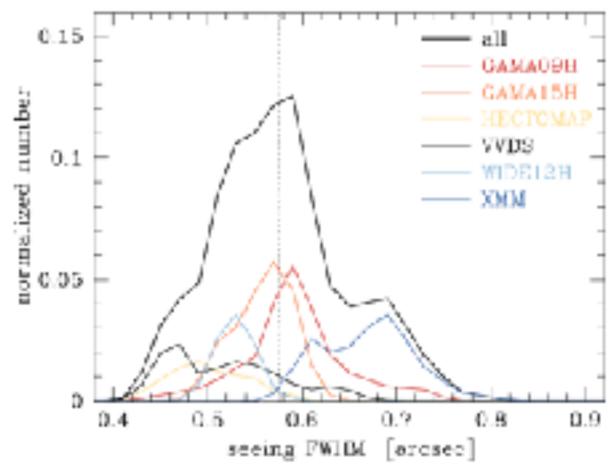

n_g ~20 arcmin^{-2}, Area ~ 137 deg^2

Shear estimation: reGaussianization (GalSim)

Cosmological constraints from HSC-SSP tomographic WL peak abundances (Liu et al. 2023)

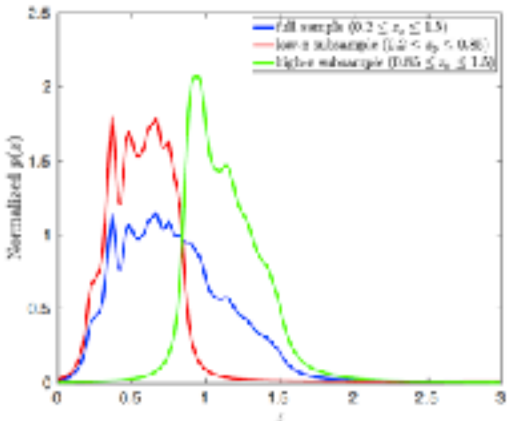

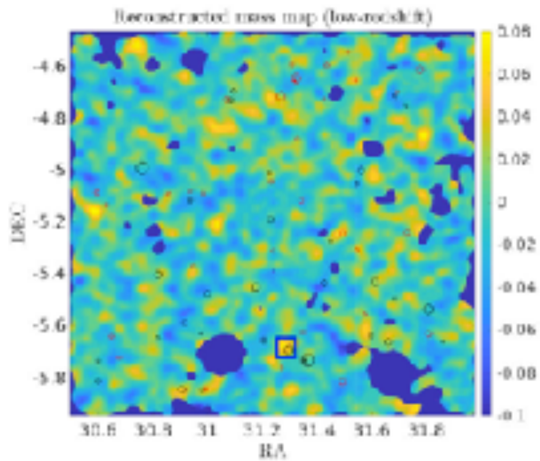

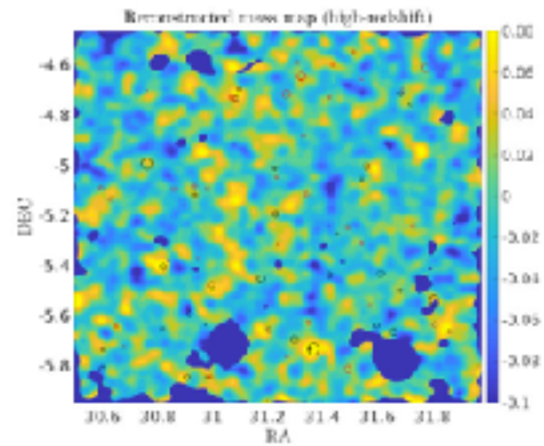

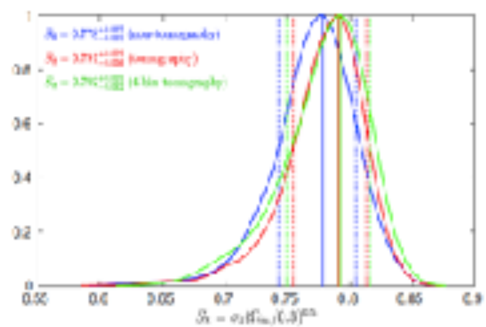

Mock simulation validation

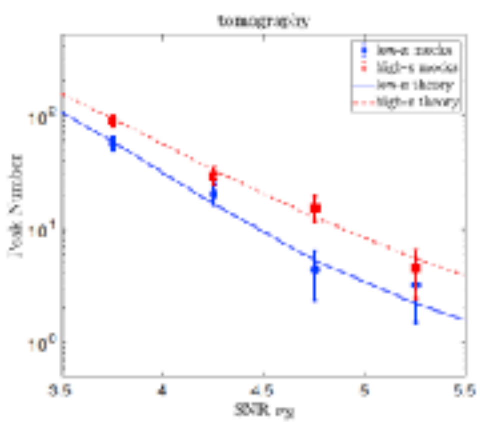

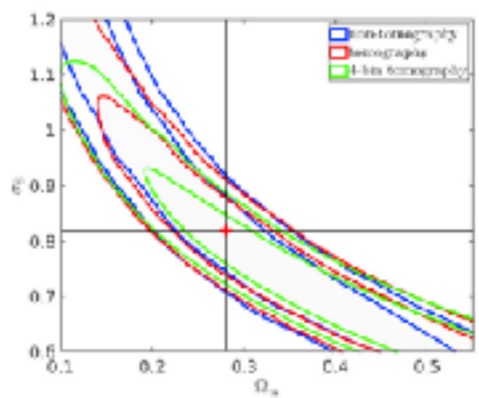

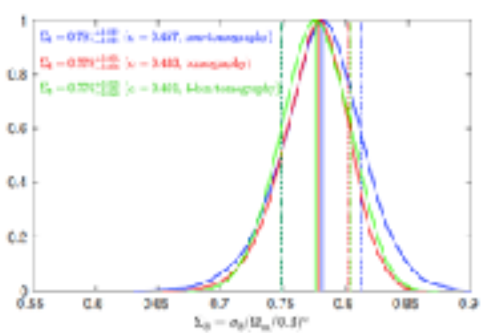

Observational analyses

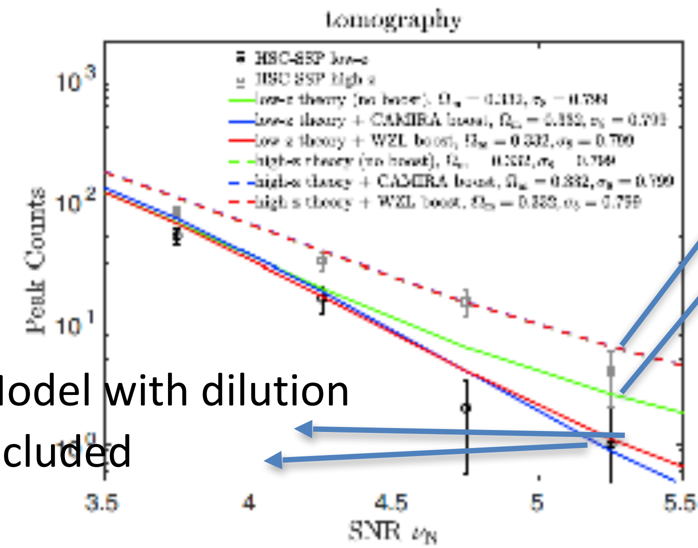

(HSC shear correlation derived) Model prediction

Model with dilution included

high-z bin → consistent well

low-z bin → data are significantly lower

→ Dilution effect: Clusters' member galaxies in the shear sample tend to bias the lensing signal of the clusters toward lower values

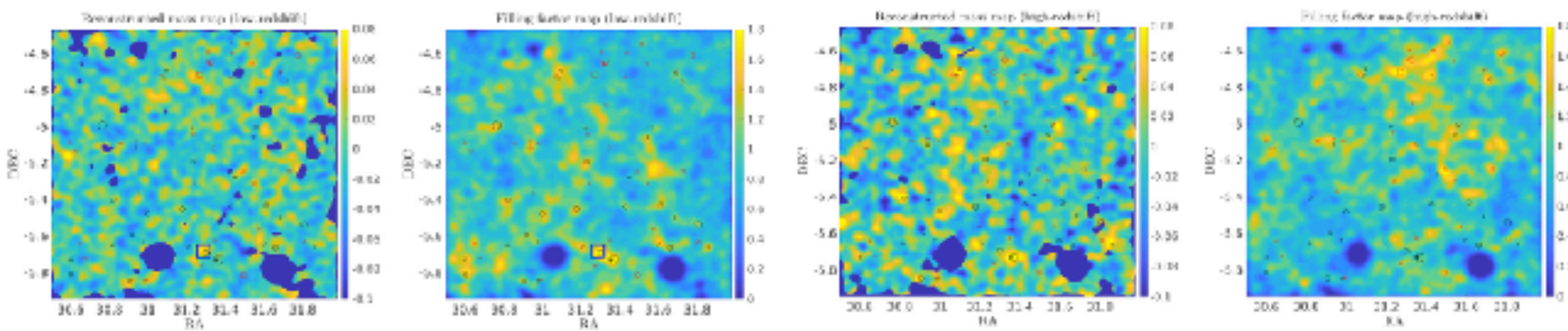

Clusters in the low-z bin contribute more to the WL peaks than the high-z ones

With clusters detected in the HSC field (Oguri et al. 2018, Wen & Han 2021), we calibrate the dilution effect and incorporate it into our theoretical model

We also analyze other systematics: photo-z, m, baryonic effect – insignificant

IA effect is less than but close to 1σ

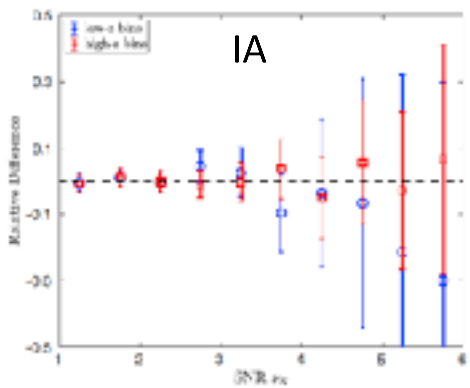

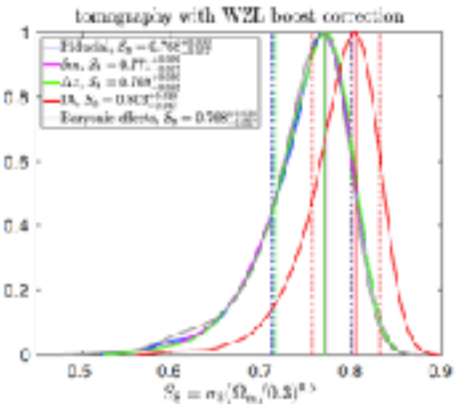

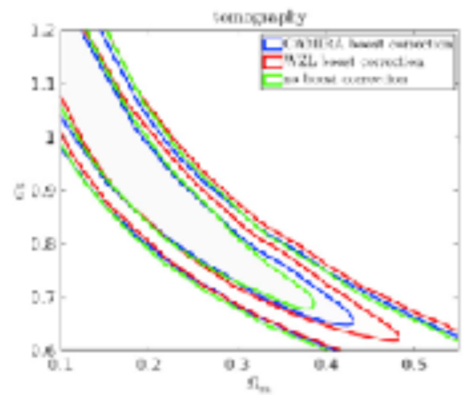

Table 2. Summary for S_8 and Σ_8 constraints of mock simulation analyses and real observations.

		S_8	Σ_8	α
Mock	Non-tomography	$0.778^{+0.037}_{-0.035}$	$0.781^{+0.032}_{-0.031}$	0.457 ± 0.014
	Tomography	$0.791^{+0.032}_{-0.036}$	$0.778^{+0.024}_{-0.025}$	0.433 ± 0.013
	Four-bin tomography	$0.797^{+0.035}_{-0.042}$	$0.776^{+0.026}_{-0.028}$	0.401 ± 0.014
Obs.	Non-tomography (CAMIRA)	$0.768^{+0.032}_{-0.043}$	$0.774^{+0.034}_{-0.040}$	0.462 ± 0.013
	Tomography (CAMIRA)	$0.758^{+0.033}_{-0.036}$	$0.772^{+0.026}_{-0.031}$	0.382 ± 0.013
	Non-tomography (WZL)	$0.770^{+0.030}_{-0.040}$	$0.752^{+0.030}_{-0.038}$	0.469 ± 0.015
	Tomography (WZL)	$0.768^{+0.030}_{-0.037}$	$0.781^{+0.026}_{-0.031}$	0.381 ± 0.012

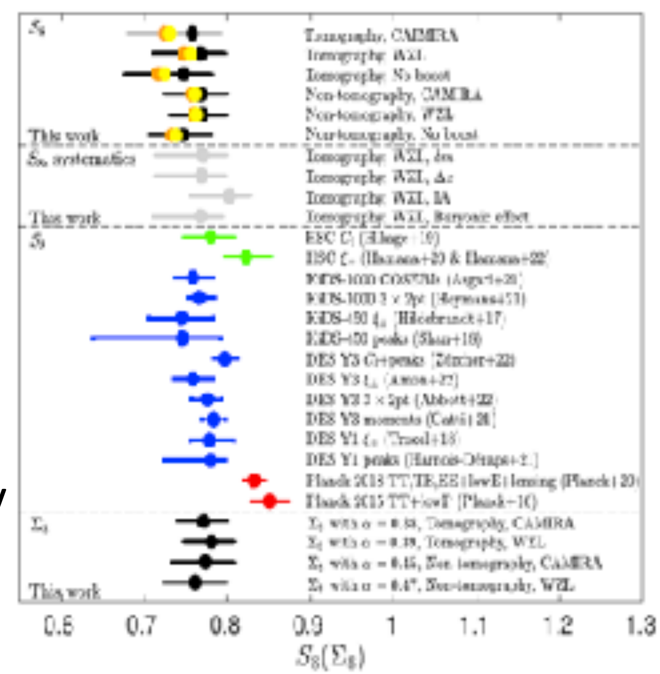

* Consistent with HSC correlation studies

* 2-bin tomography → reduce the uncertainty of $\Sigma_8 = \sigma_8(\Omega_m/0.3)^\alpha$ ($\alpha \approx 0.38$) by a factor of ~1.3

* Dilution and IA are becoming important

➢ IA impacts on WL peak statistics (Zhang et al. 2022)

Using cosmological simulations with semi-analytical galaxy formation (Wei et al. 2018)

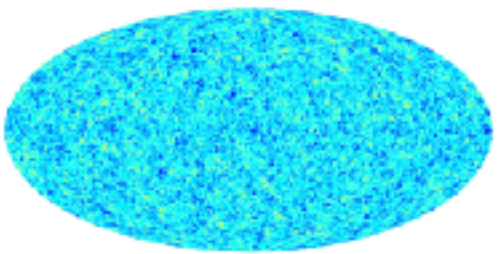

Central and satellite galaxies (Guo et al. 2013, Luo et al. 2016)

Bulge to total flux ratio B/T>/<0.6 → early/late type galaxies

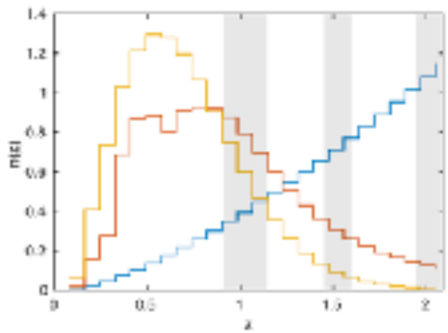

Blue is the redshift distribution of the parent galaxy sample →from that we select galaxies with different redshift distributions (red: Euclid-like, yellow: KiDS-like).

Central IA – given by the simulation

We change satellite IA to study their impacts on WL peaks

High-IA : radially aligned satellites

Low-IA: randomly orientated satellites

$$f(\theta_{3D})d\theta_{3D}\,d\phi = A\exp\left[-\frac{1}{2}\left(\frac{\theta_{3D}-\theta_0}{\sigma_\theta}\right)^2\right]d\theta_{3D}\times\sin(\theta_{3D})d\phi$$

How do the IA effects arise?

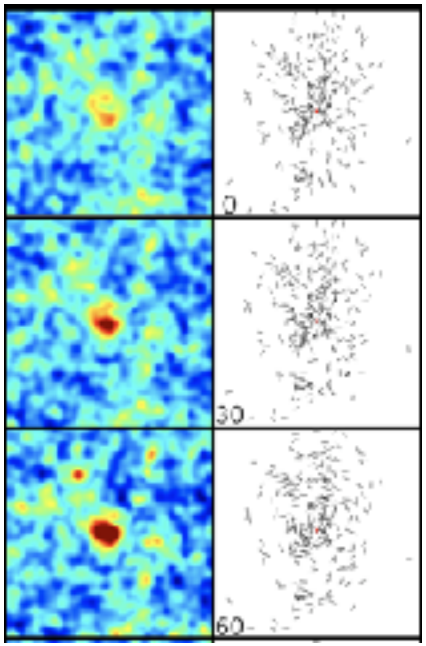

Source sample contains cluster member galaxies
→Affect their host cluster peak signals
→Closely related to the dilution effect

High peaks are affected more significantly
For Euclid-like, ~20-40% decrease of peaks with S/N>~4 for σ_θ ~40^o-80^o

Matched peak comparison

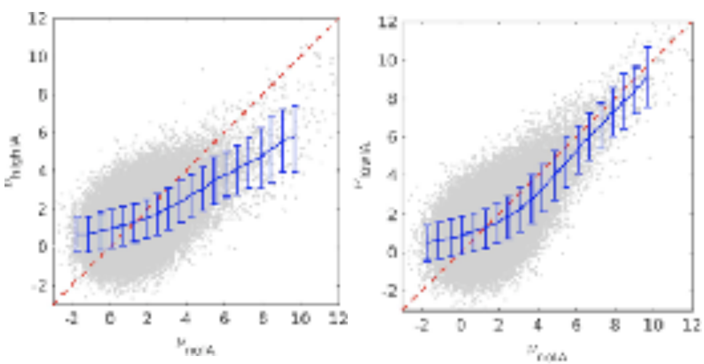

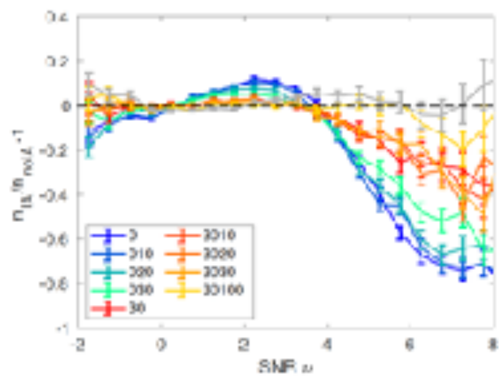

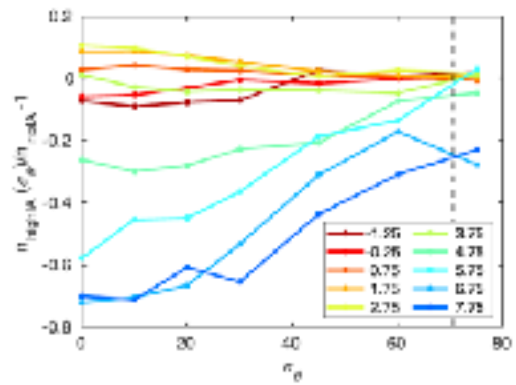

For source galaxies in narrow redshift bins

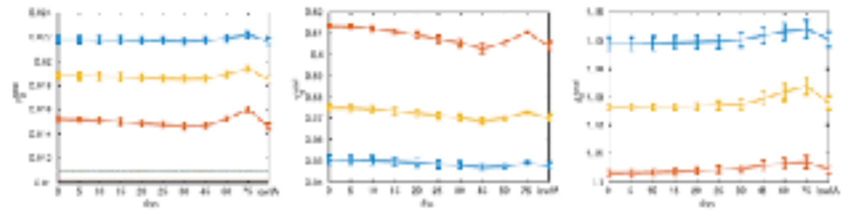

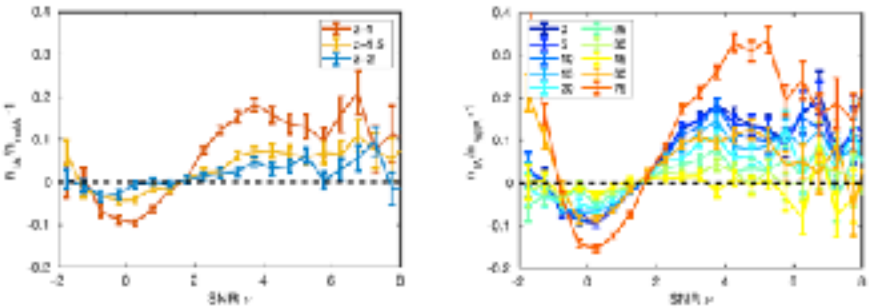

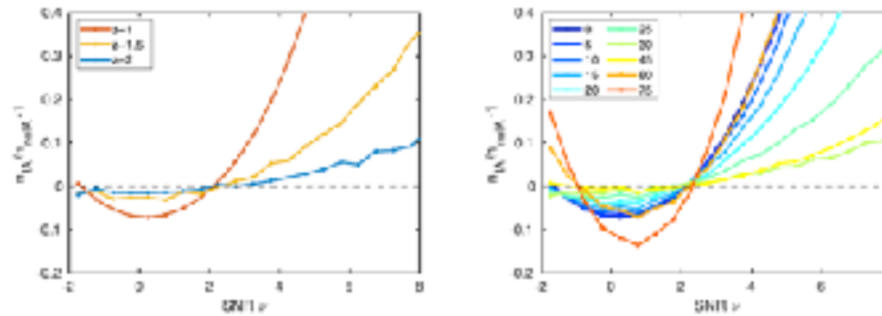

Pure Gaussian model comparisons

-- The behaviors are different: satellite IA affects cluster WL signals insignificantly because no foreground cluster members are in the source sample

-- IA contributes (both central and satellite) additional noise → affects peak statistics

Summary of IA effects on WL peaks

-- Decrease cluster WL signals because of their members in the shear sample

-- Change the noise properties

-- Ongoing study to incorporate IA into our model

-- reduce the cosmological bias

-- constrain IA simultaneously, particularly satellite IA

➢ WL peak steepness statistics (Li et al. et al. 2023)

With machine learning, In Ribli et a. 2019a, they analyzed the WL convergence map features, and found that the statistics of steepness of WL peaks carry additional cosmological information in comparison with the peak height statistics

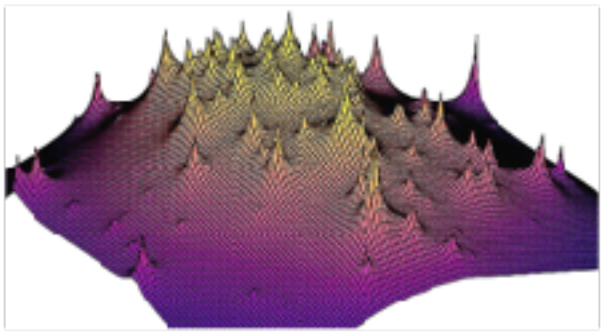

Mathematically, for a peak, its first derivatives are zero by definition. Thus the steepness of a peak is reflected by its second derivatives

With ray-tracing simulations, we analyze the two statistics systematically, and also put forward a theoretical model for high peak steepness abundances

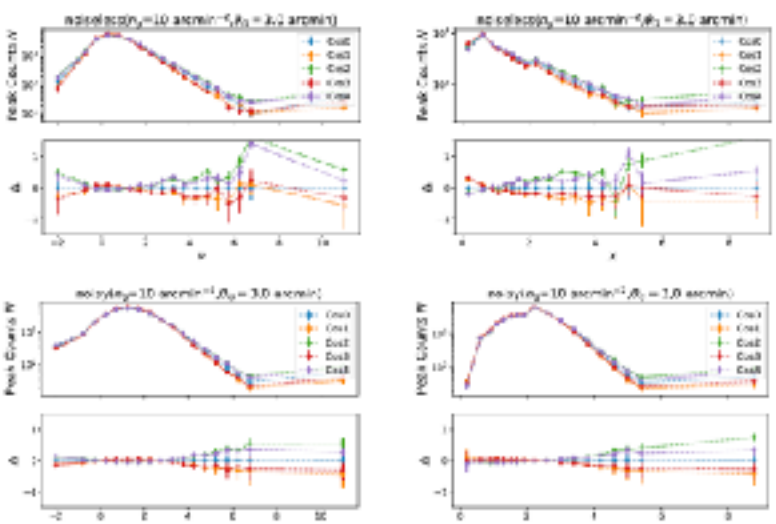

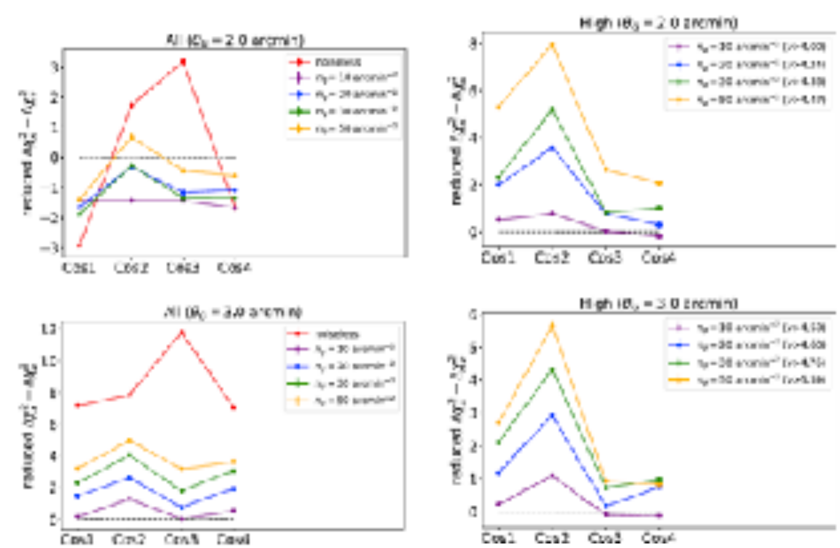

Fisher analyses: steepness statistics is more informative at low noise cases

All peaks

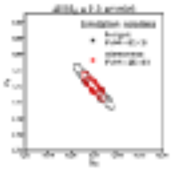

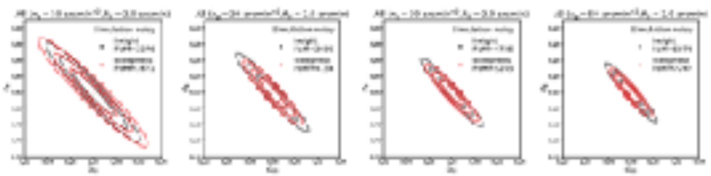

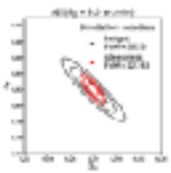

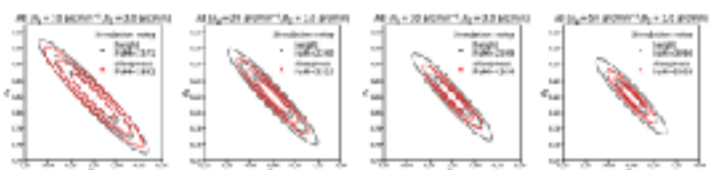

High peaks

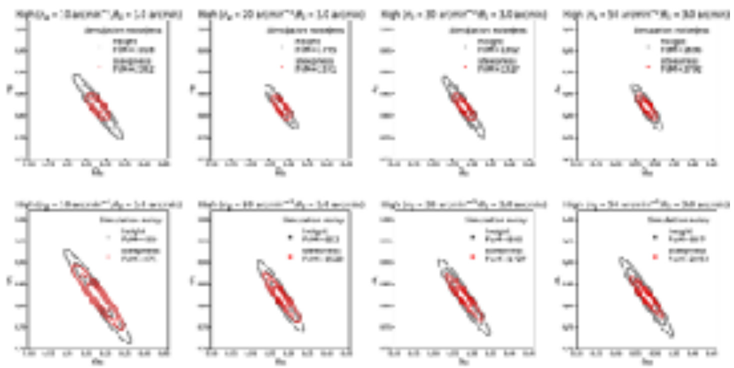

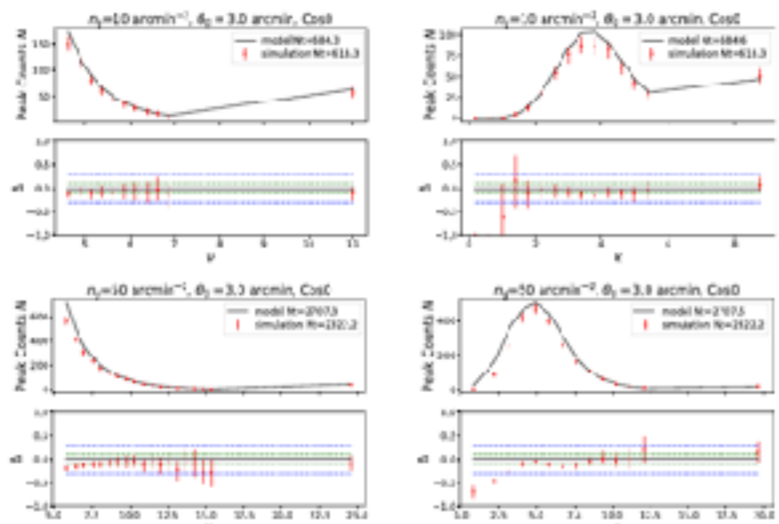

Similar halo model but for the second derivatives x – works well for high peaks

Different sensitivities to the physical parameters (from our model)

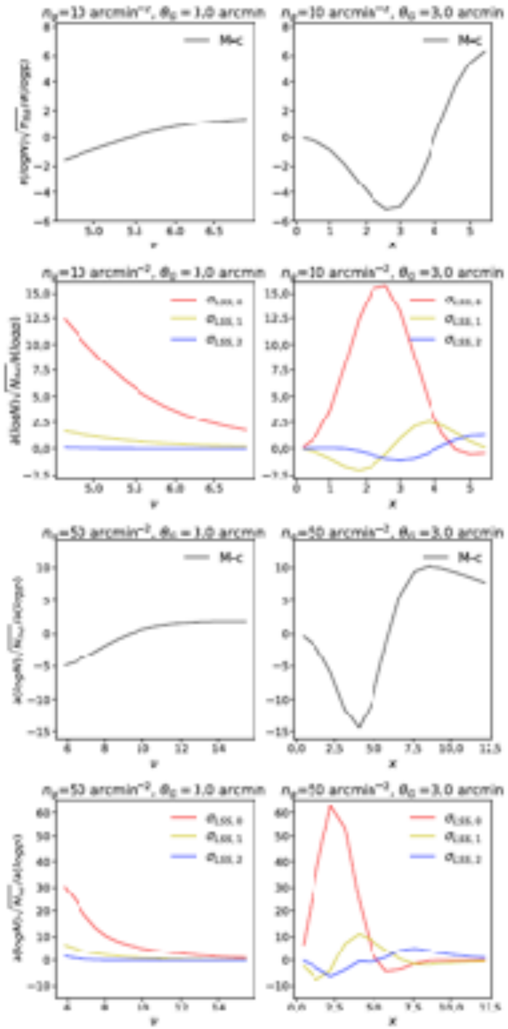

More sensitive to halo profile (M-c)
More sensitive to LSS projection effects (cosmological info.)

In addition to cosmological constraints, steepness statistics might be a better probe to study the baryonic effects on halos (through the change of M-c relation)

We are currently working on the first application of the WL peak steepness analyses to HSC data.
The mock results are encouraging (Li et al. inpreparation)

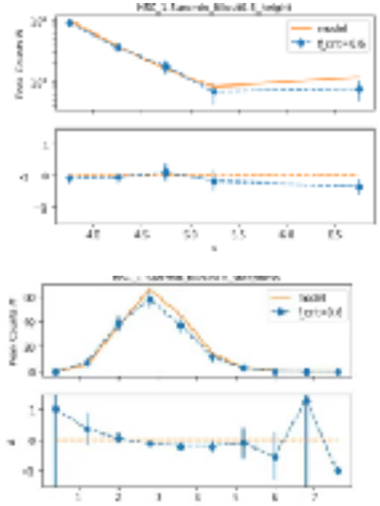

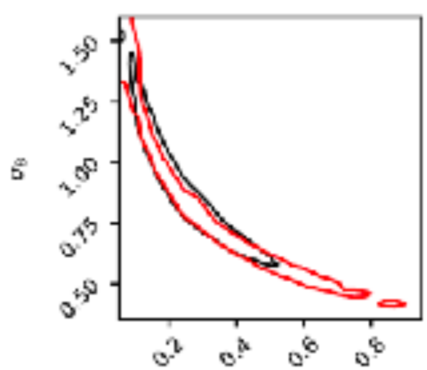

Black: peak height
Red: peak steepness

- **First detection of cosmic magnification via shear-position correlation from HSC (Liu et al. 2021)**

Two-side of the WL: shear and magnification that induces extra clustering

Cross-correlation of kappa-maps from shear measurements with far-away galaxy number distributions

□ □ □ □ □ →□ extract magnification effect
(nearly) : independent of galaxy intrinsic clustering and bias

□ □ □ □ □ →□ calibrate shear measurement errors

Cross-correlation of kappa-maps from shear measurements with far-away galaxy number distributions

$$\delta_{ng} = \delta_{ng}^{\mathrm{int}} + \delta_{\mu}$$

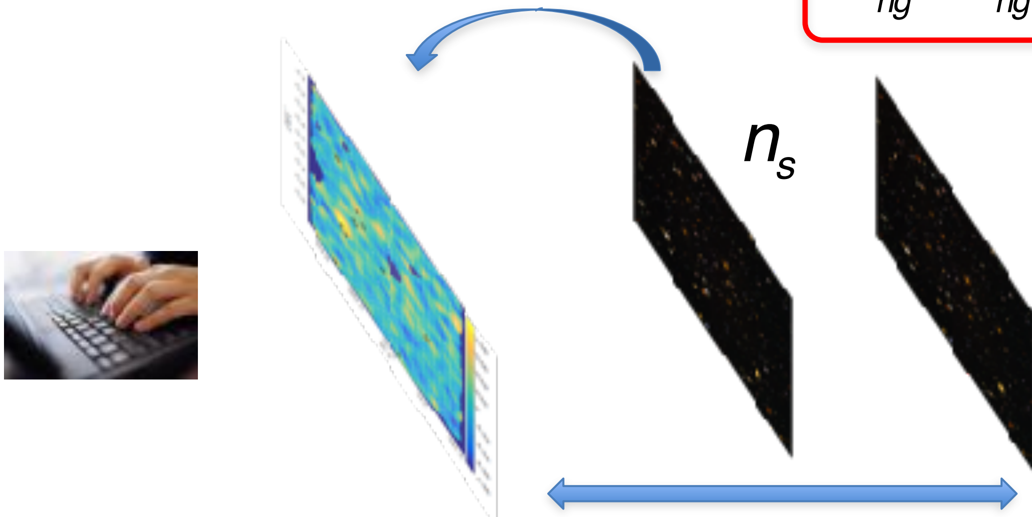

$$\delta_{\mu j}(\hat{\mathbf{n}}', m_{lim}) = \mu^{\alpha(m_{lim})-1} - 1$$

$$\alpha(m_{lim}) = 2.5\mathrm{d}[\log_{10} N(m_{lim})]/\mathrm{d}m$$

$$\kappa \ll 1, \mu \approx 1 + 2\kappa$$

$$\delta_{\mu j}(\hat{\mathbf{n}}', m_{lim}) = 2\kappa_j(\hat{\mathbf{n}}')[\alpha(m_{lim}) - 1]$$

$$< \kappa(z_f)\delta_{ng}(z_b) > = < \kappa(z_f)\delta_{ng}^{\mathrm{int}}(z_b) > + < \kappa(z_f)\delta_{\mu}(z_b) >$$
$$\approx < \kappa(z_f)\delta_{\mu}(z_b) >$$

$$\omega_{ij}(\theta) = \langle 2[\alpha(m_{lim}) - 1]\kappa_i(\hat{\mathbf{n}})\kappa_j(\hat{\mathbf{n}}')\rangle_\theta$$
$$= 2[\alpha(m_{lim}) - 1]\frac{1}{2\pi}\int_0^\infty l\mathrm{d}l P_\kappa^{ij}(l) J_0(l\theta).$$

$\kappa(z_f)$: from shear measurement of $n_{s,}$

$\delta_\mu(z_b)$: magnification induced clustering for galaxies brighter than a *mag* threshold

→ Such a measurement is independent of galaxy bias if the background and foreground are well separated.

We combine the HSC Year 1 shear catalog and DR2 photometric catalog

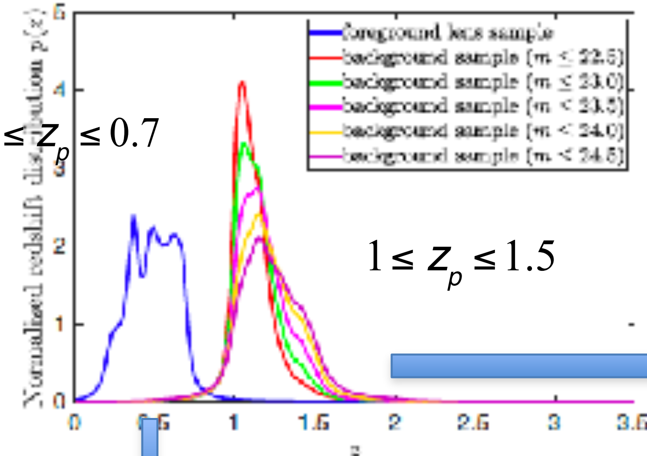

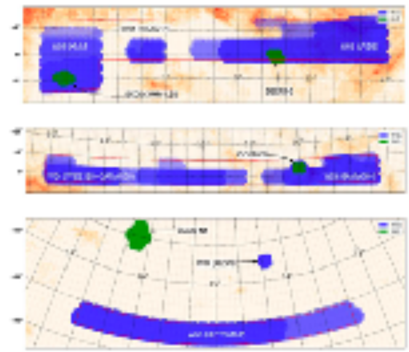

Aihara, H. et al. 2019, PASJ, 71, 114

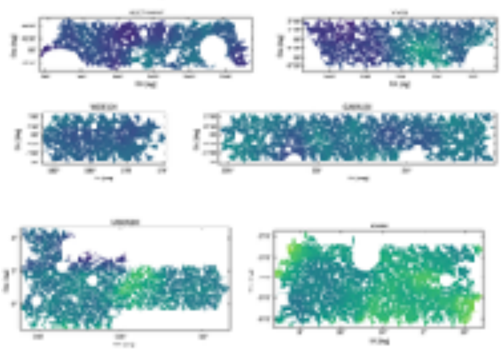

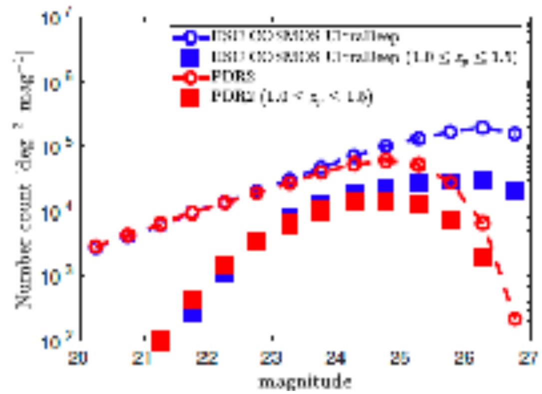

mag limit	22.5	23	23.5	24	24.5
α	2.48	1.97	1.48	1.14	0.85

Convergence fields
Overlapped region with DR2 and remove masks and boundaries
→ ~60 deg^2

Complete up to mag ~25
We construct subsamples with different mag cuts

First detection of the cross correlations

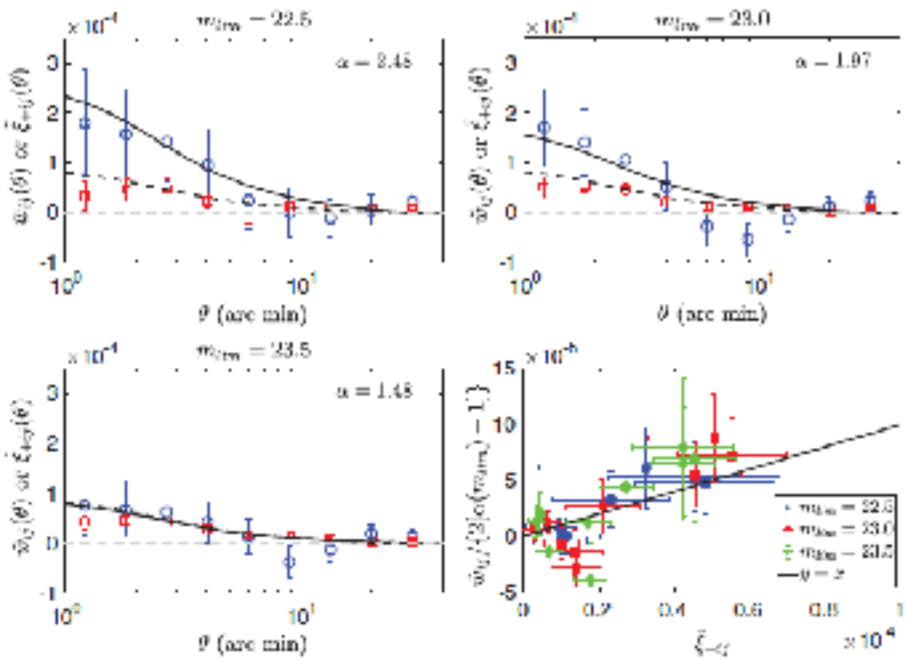

Mathematically (A=2(α-1))

$$\frac{<\kappa(z_f)\delta_\mu(z_b)>}{<\gamma(z_f)\gamma(z_b)>} = \frac{w_{ij}(\theta)}{\zeta_+(\theta)} \sim \frac{A}{(1+m)}$$

With $\begin{pmatrix} w_{ij}(\theta) \\ \zeta_+(\theta) \end{pmatrix}$

we can constrain shear bias m using data along independent of cosmology

→Potential to extend 3×2pt

Magnification-induced systematics

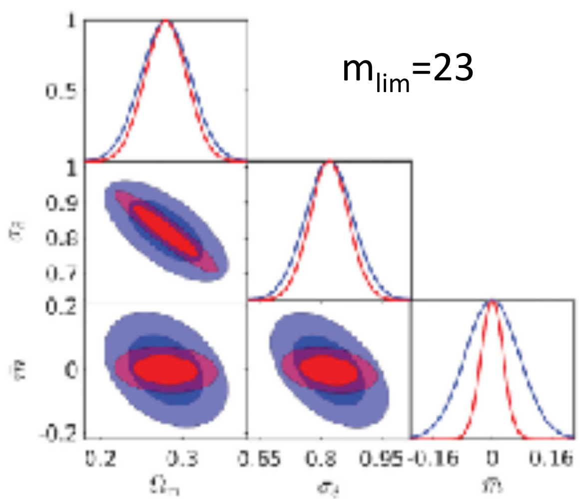

m_{lim}=23

CSST or Euclid-like surveys

TABLE I. Forecast constraints for a 15000 deg^2 survey.

	SS only	SS and SP
Ω_m (68% C.L.)	0.032	0.027
σ_8 (68% C.L.)	0.059	0.051
$\bar{m}$ (68% C.L.)	0.075	0.032
S_8 (68% C.L.)	0.043	0.020

- **Summary and discussion**

➢ Statistics beyond 2pt statistics are important in WL cosmology
➢ WL peak statistics are complementary means to probe non-Gaussian info.
➢ Peak steepness statistics is new and deserves further studies
➢ Investigations of systematic effects

➢ shear-position correlations can be important to constrain the shear bias and to extend 3×2pt analyses

➢ Stage IV surveys are coming soon (Euclid is in orbit already)
Explore the synergy is important

Potential synergy between CSST and Euclid in WL cosmology (Liu,D.Z. et al. 2023)

CSST and Euclid will survey nearly the same sky area of about 15000 deg^2 with similar high resolutions, but the bands are different

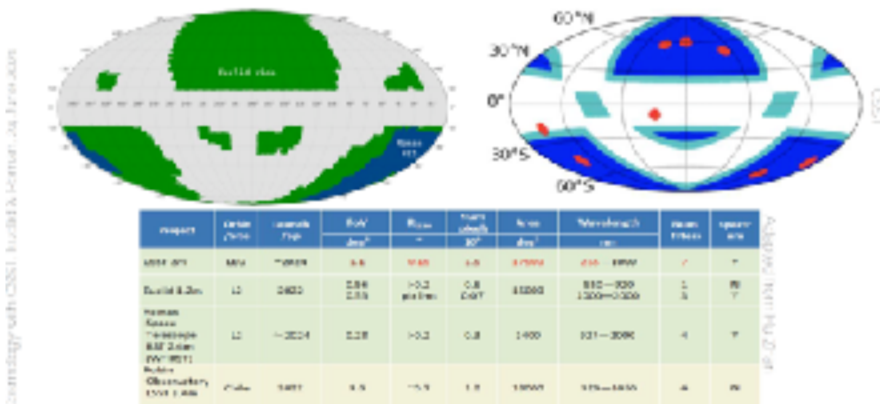

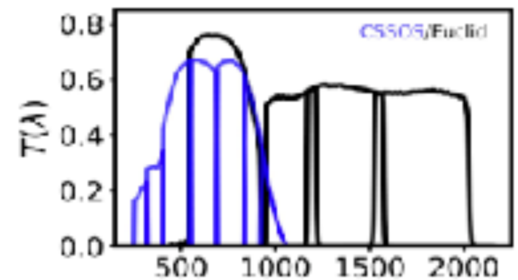

Table 1. Photo-z statistics in different cases.

Combination	Bias	σ_{NMAD}	η
CSST-only	+0.0043	0.048	8.45%
Euclid+CSST	−0.0051	0.036	2.35%
Euclid+LSST-like	−0.0019	0.018	0.82%
Euclid+DES-like	−0.0057	0.054	12.87%

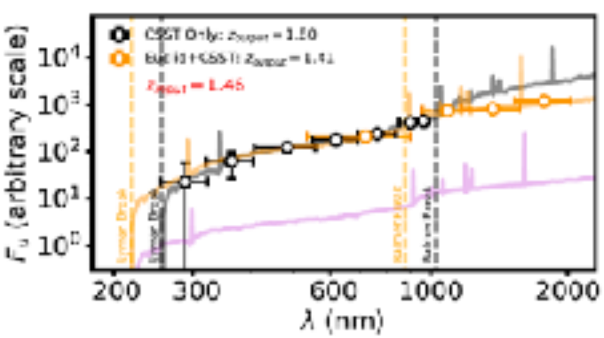

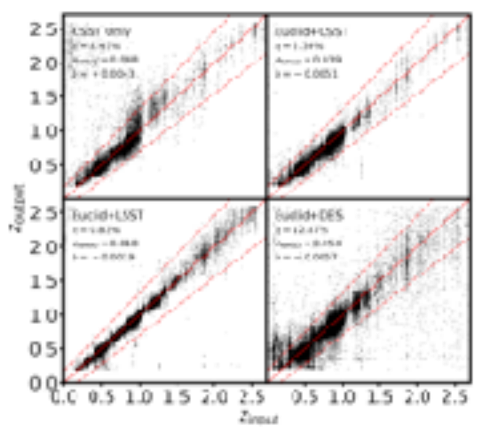

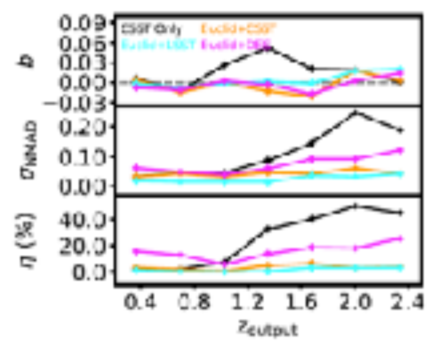

Thank you